Resource-efficient linear-optical quantum router

Karel Lemr,[1,*] Karol Bartkiewicz,[1] Antonín Černoch,[1] and Jan Soubusta[2]

[1]*RCPTM, Joint Laboratory of Optics of Palacký University and Institute of Physics of Academy of Sciences of the Czech Republic,*
17 listopadu 12, 772 07 Olomouc, Czech Republic

[2]*Joint Laboratory of Optics of Palacký University and Institute of Physics of Academy of Sciences of the Czech Republic, 17 listopadu 50A,*
779 07 Olomouc, Czech Republic

An all-linear-optical scheme for a fully featured quantum router is presented. This device directs the signal photonic qubit according to the state of one control photonic qubit. In the introduction we formulate the list of requirements imposed on a fully quantum router. Then we describe our proposal, showing the exact principle of operation on a linear-optical scheme. Subsequently we provide a generalization of the scheme in order to optimize the success probability by means of a tunable controlled-phase gate. Finally, we show how one can modify the device to route multiple signal qubits using the same control qubit.

PACS number(s): 03.67.Hk, 42.50.Dv, 03.67.Lx

I. INTRODUCTION

Quantum communications represent a very important part of a rapidly developing research area called quantum information processing [1,2]. Communications networks are now an indispensable technology allowing people to transmit information quickly over large distances. In classical communications networks laws of classical physics are used to govern their operation. Recent research in quantum physics and quantum information suggests that quantum laws of nature can provide significant improvement of capabilities of communications devices [3–5], while using similar resources and keeping similar network architecture [6,7]. Not surprisingly, a significant amount of theoretical and experimental research has been dedicated to the concept of quantum communications networks [8]. The most notable result of this effort is a number of protocols for quantum cryptography [9,10], which is a method for unconditionally secure transmission of information using various quantum properties of information carriers. Quantum communications networks can benefit from purely quantum effects such as entanglement or the probabilistic nature of measurement.

The more complex both the classical and quantum networks are, the more pronounced is the need for correct routing of the signal from its source to its intended destination [11,12]. Classical routers are well-known ingredients of classical networks allowing one to direct signal information according to control information (e.g., IP address) [13]. The analogy between classical and quantum networks suggests that complex quantum networks would also require elaborate routing protocols. This need is even more pronounced since in contrast to classical information one cannot perfectly duplicate an unknown qubit of quantum information [14]. However, approximate cloning is possible and has been intensely studied both theoretically and experimentally over the last decades [15–17], resulting in, e.g., establishing and implementing optimal state-dependent cloning for a wide class of qubit distributions [18,19]. Nevertheless the impossibility of perfect cloning prevents using the concept of multidirectional broadcast (known from classical networks) in a quantum network.

In this paper we address the problem of designing a quantum router (see the conceptional scheme in Fig. 1). We consider the platform of individual photons and linear optics because of its experimental accessibility and also because of the particular suitability of light for information transmission [20]. The router has to fulfill five requirements to be suitable for quantum communications networks:

(1) Both the signal and control information have to be stored in quantum objects (qubits), and therefore routers using classical information to route the quantum signal are considered only semiquantum routers.

(2) The signal information is unchanged under the routing operation; the degree of freedom used to store the signal qubit information has to be kept undisturbed.

(3) The router has to be able to route the signal into a coherent superposition of both output modes.

(4) The router has to work without any need for postselection on the signal output. If the router is probabilistic, successful operation can be identified by detection on the control state.

(5) To optimize the resources of the quantum network, only an individual control qubit is required to direct one signal qubit.

There have been several schemes for quantum routers already proposed; some of them have been experimentally implemented, but none of them meets all five requirements defined in the above paragraph. The first group of these proposals uses light-matter interaction in order to achieve quantum routing [21–23]. Such interaction is, however, often very challenging for experimental implementation. The second group of the proposals considers solely the platform of optical interactions to accomplish the routing. There are some proposals for a semiquantum router, where the control information is classical using intensive light pulses [24]. There are also proposals in which the control information is quantum, but the signal state collapses in the router so requirement 2 is not met [25]. Recently we have proposed a fully quantum router using only linear optics [26]. This device, however, does not meet requirement 5 since it requires two quantum bits to control routing of one single qubit of signal information.
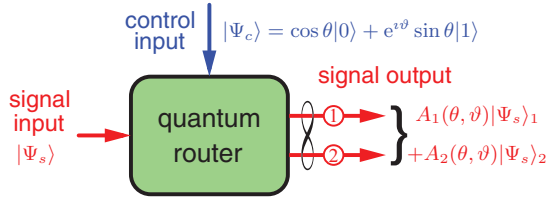
*k.lemr@upol.cz

FIG. 1. (Color online) Conceptual scheme of a quantum router.

II. PRINCIPLE OF OPERATION

In this section we describe an all-linear-optical quantum router that meets all five requirements mentioned in the introduction. The router makes use of three quantum gates: controlled-phase gate (c-phase gate) [28–32], quantum nondemolition presence detection gate (QND gate) [33], and programmable-phase gate (PPG) [34–36]. In order for the setup to work completely without the need for signal postselection, both the QND and the detector D have to be equipped with photon-number resolving detectors. Without them, the router still works but does not fulfill requirement 4. Linear-optical schemes of all of these gates are already published and with the exception of the QND gate are also already tested experimentally. The reader is encouraged to get more details in the cited papers. Figure 2 shows the scheme for linear-optical implementation of the quantum router. We propose using two degrees of freedom of individual photons: (1) polarization encoding, used to store both the signal and control qubits, and (2) path (spatial mode) encoding, used
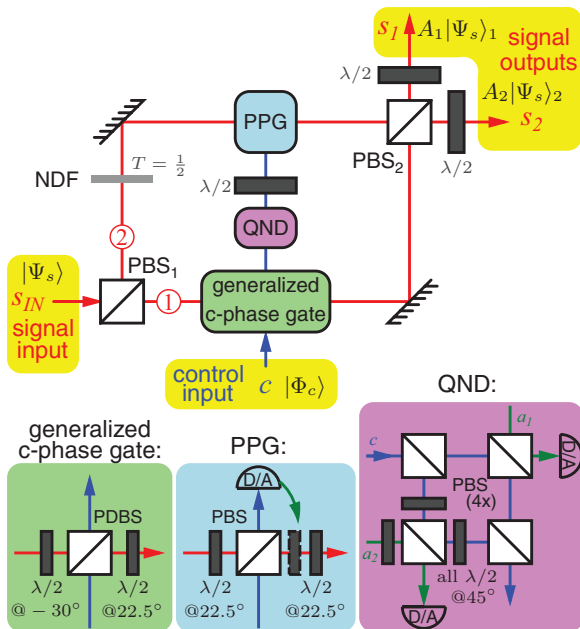

FIG. 2. (Color online) Scheme of the linear-optical implementation of a quantum router. PBS denotes polarizing beam splitter, PDBS denotes polarization dependent beam splitter, $\lambda/2$ and $\lambda/4$ denote half- and quarter-wave plates, NDF denotes neutral-density filter, c-phase denotes controlled phase gate, QND denotes quantum nondemolition detector, PPG denotes programmable-phase gate, and D/A denotes polarization analysis (for more details see Ref. [27]). Red lines depict signal modes, while blue lines depict control modes.

for the routing operation; the signal photon is routed into superposition of two output ports.

The signal qubit enters the setup using the input port s_{in}, while the control qubit enters the router using port c. Let us assume the signal qubit takes the form of a general quantum polarization state:

$$|\Psi_s\rangle = \alpha|H\rangle + \beta|V\rangle, \tag{1}$$

where $|H\rangle$ and $|V\rangle$ denote the states of horizontal and vertical linear polarizations and $|\alpha^2| + |\beta^2| = 1$. For reasons apparent later, it is suitable to parametrize the state of the control qubit by angles θ and ϑ:

$$|\Psi_c\rangle = \cos\theta|H\rangle + e^{\iota\vartheta}\sin\theta|V\rangle. \tag{2}$$

After the signal qubit enters the router, it is subjected to the polarizing beam splitter (PBS$_1$) transmitting horizontally polarized light and reflecting light of vertical polarization. At this point the state of both signal and control qubits reads

$$|\Psi_s\rangle \otimes |\Phi_{c1}\rangle = \alpha\cos\theta|H_1 H_c\rangle + \alpha e^{\iota\vartheta}\sin\theta|H_1 V_c\rangle$$
$$+ \beta\cos\theta|V_2 H_c\rangle + \beta e^{\iota\vartheta}\sin\theta|V_2 V_c\rangle, \tag{3}$$

where indices denote spatial modes of the qubits.

For better readability, let us now consider the evolution of both arms of the interferometer (labeled in Fig. 2 as ① and ②) separately starting with the lower arm ① corresponding to the first two terms in Eq. (3): The horizontally polarized signal photon undergoes a generalized Hadamard transformation on a half-wave plate (HWP) rotated by $-30°$ [1]:

$$|H_1\rangle \rightarrow \frac{1}{2}|H_1\rangle - \frac{\sqrt{3}}{2}|V_1\rangle.$$

Subsequently both the signal and control qubit photons enter the c-phase gate implemented using polarization dependent beam splitter (PDBS) of intensity transmissivities $T_V = \frac{1}{3}$ and $T_H = 1$ for vertical and horizontal polarization, respectively. Postselecting only on the cases in which there is one photon in signal and one photon in control mode, the transformation performed by the c-phase gate renders the investigated first two terms of Eq. (3) to

$$\frac{\alpha\cos\theta}{2}(|H_1\rangle + |V_1\rangle)|H_c\rangle + \frac{\alpha e^{\iota\vartheta}\sin\theta}{2\sqrt{3}}(|H_1\rangle - |V_1\rangle)|V_c\rangle.$$

In the next step, the signal qubit undergoes Hadamard transform also using a HWP yielding the terms

$$\frac{\alpha\cos\theta}{\sqrt{2}}|H_1 H_c\rangle + \frac{\alpha e^{\iota\vartheta}\sin\theta}{\sqrt{6}}|V_1 V_c\rangle.$$

As mentioned above, the c-phase gate is successful only when the signal and control qubits leave the gate by separate output ports. In order to postselect only on such cases, the control qubit has to be subjected to QND presence detection via the QND gate. The QND presence detection requires an entangled pair of photons as a resource, but these photons are of a fixed quantum state, are generated locally solely for the purposes of

---

[1]In the entire paper, rotations of wave plates are given as the angle between the optical axis of the wave plate and the direction of horizontal linear polarization.

the QND gate, and do not take another part in the quantum network. The control qubit state does not change under the QND gate, but a success probability factor of $\frac{1}{2}$ is added to take into account the success probability of the QND gate. More information about the QND gate can be found in Ref. [33]. In the last step, the control qubit is subjected to a half-wave plate rotated at 22.5° yielding the terms

$$\frac{\alpha\cos\theta}{2\sqrt{2}}|H_1\rangle(|H_c\rangle + |V_c\rangle) + \frac{\alpha e^{\iota\vartheta}\sin\theta}{2\sqrt{6}}|V_1\rangle(|H_c\rangle - |V_c\rangle),$$

and then the control qubit alone impinges on the PPG composed only of a PBS. The PPG gate heralds successful operation only if there is a control qubit with horizontal polarization at its input, thus projecting the signal in the lower arm ① onto

$$\frac{\alpha\cos\theta}{2\sqrt{2}}|H_1\rangle + \frac{\alpha e^{\iota\vartheta}\sin\theta}{2\sqrt{6}}|V_1\rangle, \tag{4}$$

and in this form it impinges on the PBS$_2$.

Now we examine the evolution of the second two terms in Eq. (3) corresponding to the propagation of the signal qubit by the upper arm ②: In this case the control qubit enters the c-phase gate alone, rendering the investigated terms to

$$\beta\cos\theta|V_2 H_c\rangle + \frac{\beta e^{\iota\vartheta}\sin\theta}{\sqrt{3}}|V_2 V_c\rangle.$$

Again, we postselect only on those cases in which the control qubit leaves the c-phase gate by the mode c. This postselection is again assured by the QND gate, which witnesses the control qubit presence with a success probability of $\frac{1}{2}$. Considering also the action of HWP we get

$$\frac{\beta\cos\theta}{2}|V_2\rangle(|H_c\rangle + |V_c\rangle) + \frac{\beta e^{\iota\vartheta}\sin\theta}{2\sqrt{3}}|V_2\rangle(|H_c\rangle - |V_c\rangle).$$

Subsequently the signal qubit undergoes a Hadamard transformation yielding

$$\frac{\beta\cos\theta}{2\sqrt{2}}(|H_2 H_c\rangle + |H_2 V_c\rangle - |V_2 H_c\rangle - |V_2 V_c\rangle)$$
$$+ \frac{\beta e^{\iota\vartheta}\sin\theta}{2\sqrt{6}}(|H_2 H_c\rangle - |H_2 V_c\rangle - |V_2 H_c\rangle + |V_2 V_c\rangle).$$

In the next step, both the signal and control qubits meet on the PPG gate's polarizing beam splitter. Since we postselect only on the cases in which there is exactly one photon at the output of mode c, we continue considering only the terms

$$\frac{\beta\cos\theta}{2\sqrt{2}}(|H_2 H_c\rangle - |V_2 V_c\rangle) + \frac{\beta e^{\iota\vartheta}\sin\theta}{2\sqrt{6}}(|H_2 H_c\rangle + |V_2 V_c\rangle).$$

As usual, the control photon impinges on the detector. Depending on the outcome of the polarizing detection measurement performed, the signal qubit collapses into

$$\frac{\beta\cos\theta}{4}(|H_2\rangle - |V_2\rangle) + \frac{\beta e^{\iota\vartheta}\sin\theta}{4\sqrt{3}}(|H_2\rangle + |V_2\rangle), \tag{5}$$

when the diagonally polarized control qubit was detected, or

$$\frac{\beta\cos\theta}{4}(|H_2\rangle + |V_2\rangle) + \frac{\beta e^{\iota\vartheta}\sin\theta}{4\sqrt{3}}(|H_2\rangle - |V_2\rangle),$$

when we observe the antidiagonally polarized control photon. In the latter case, we do apply a feedforward consisting of a HWP placed at 0° causing $|V_2\rangle \rightarrow -|V_2\rangle$ and thus correcting the signal to the form of Eq. (5). The subsequent Hadamard gate renders the signal to the form of

$$\frac{\beta e^{\iota\vartheta}\sin\theta}{2\sqrt{3}}|H_2\rangle + \frac{\beta\cos\theta}{2}|V_2\rangle.$$

Before the signal impinges on the second polarizing beam splitter PBS$_2$, we introduce filtering by a neutral-density filter (NDF) of transmissivity $T = \frac{1}{2}$ to balance the amplitude with respect to the lower arm contribution described in Eq. (4).

After having both the terms of Eq. (3) evaluated, let us recall that the total state of the signal qubit reads

$$|\Psi_s\rangle = \frac{\alpha\cos\theta}{2\sqrt{2}}|H_1\rangle + \frac{\alpha e^{\iota\vartheta}\sin\theta}{2\sqrt{6}}|V_1\rangle$$
$$+ \frac{\beta e^{\iota\vartheta}\sin\theta}{2\sqrt{6}}|H_2\rangle + \frac{\beta\cos\theta}{2\sqrt{2}}|V_2\rangle,$$

and after being subjected to the PBS$_2$ it takes the form of

$$|\Psi_s\rangle = \frac{\cos\theta}{2\sqrt{2}}(\alpha|H_1\rangle - \beta|V_1\rangle) + \frac{e^{\iota\vartheta}\sin\theta}{2\sqrt{6}}(\beta|H_2\rangle + \alpha|V_2\rangle).$$

The additional half-wave plate at 0° in the first output corrects $-V \rightarrow +V$, and polarization swap $H \leftrightarrow V$ is applied to the second output by inserting a half-wave plate at 45° yielding the final form of the signal state at the output of the router:

$$|\Psi_s\rangle_{\text{out}} = A_1|\Psi_s\rangle_1 + A_2|\Psi_s\rangle_2, \tag{6}$$

where one can clearly observe the routing operation. The polarization state remains in the original form of Eq. (1), but the spatial degree of freedom is modified depending on the parameter θ of the control qubit. The ratio between the amplitudes A_2 and A_1 depends straightforwardly on this parameter:

$$\tan\chi = \frac{|A_2|}{|A_1|} = \frac{\tan\theta}{\sqrt{3}}, \tag{7}$$

where we have introduced the routing ratio parameter χ in a similar manner as splitting ratio parametrization is introduced for ordinary beam splitters. Since θ lies in the interval $[0; \frac{\pi}{2}]$, the router can direct all the signal to the first output (A_1), to the second output (A_2), or to any of their superposition.

The success probability $P_{\text{succ}} = |A_1|^2 + |A_2|^2$ does not depend on the signal state parameters α and β but only on the ratio χ and therefore on the control qubit parameter θ. One can easily find the relation between success probability and the routing parameter χ or the control qubit parameter θ:

$$P_{\text{succ}} = \frac{1 + 2\cos^2\theta}{24} = \frac{1 + \tan^2\chi}{8 + 24\tan^2\chi}. \tag{8}$$

It reaches a maximum of $\frac{1}{8}$ for $\chi = \theta = 0$, and, on the other hand, it is minimized for $\chi = \theta = \frac{\pi}{2}$ to a value of $\frac{1}{24}$. The plot in Fig. 3 shows the success probability of routing as a function of the routing parameter χ. It also depicts the relation between the routing parameter χ and the control qubit parameter θ.

Note that the neutral-density filter of the intensity transmissivity of $\frac{1}{3}$ can be placed to output port s_1 in order to
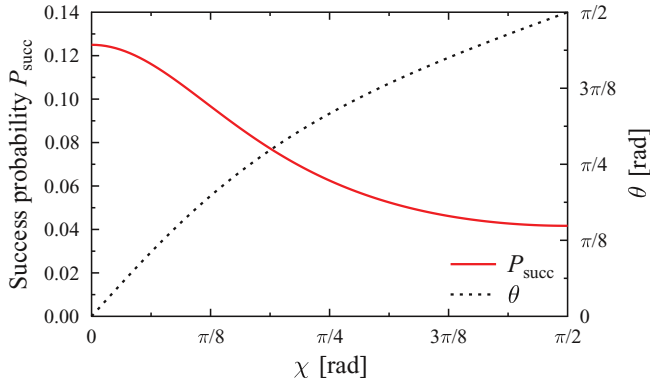
FIG. 3. (Color online) Success probability of the routing procedure as a function of the routing ratio parameter χ. Additionally the plot shows the relation between the routing parameter χ and the control qubit parameter θ.

equalize the success probability so it is completely control state independent and fixed to the value of $\frac{1}{24}$.

III. TUNABLE C-PHASE GATE BASED ROUTER

In the previous section we have considered only the c-phase gate with a fixed phase shift of $\varphi = \pi$ (also known as the controlled-sign gate). In some cases, however, higher success probability can be achieved using a tunable c-phase gate that can be set to exercise a phase shift φ of any value in the range $[0; \pi]$. The reason for considering this tunable c-phase gate lies in the fact that the success probability of the gate is a function of its phase shift. In 2010, Konrad Kieling and his colleagues [30] discovered the success probability P_C relation to the phase shift φ [2]:

$$P_{\mathrm{C}} = \left[1 + 2\left| \sin\frac{\varphi}{2} \right| + 2^{3/2} \sin\left(\frac{\pi - \varphi}{4}\right) \left| \sin\frac{\varphi}{2} \right|^{1/2} \right]^{-2}. \quad (9)$$

In order to make the c-phase gate tunable, one needs to replace the fixed polarization dependent beam splitter by an interaction Mach-Zehnder interferometer with tunable phase and losses [see Fig. 4(a)].

In a recent paper [32], we showed that if one does not seek this success probability to be input state independent the c-phase gate can be generalized to perform the transformation

$$|H_1 H_c\rangle \to |H_1 H_c\rangle, \quad |H_1 V_c\rangle \to \sqrt{A_C}|H_1 V_c\rangle,$$
$$|V_1 H_c\rangle \to \sqrt{A_C}|V_1 H_c\rangle, \quad |V_1 V_c\rangle \to A_C e^{\iota\varphi}|V_1 V_c\rangle,$$
$$|V_2 H_c\rangle \to |V_2 H_c\rangle, \quad |V_2 V_c\rangle \to \sqrt{A_C}|V_2 V_c\rangle, \quad (10)$$

where we have already adopted the notation of Eq. (3) and introduced $|A_C|^2 = P_C$. Note that in the first and fifth cases there is no photon entering the interaction interferometer, while in the second, third, and sixth cases there is exactly one photon entering this interferometer. In the fourth case, both the photons are subjected to the interferometer. The success probability thus becomes input state dependent but higher in average.

_____

[2] P_C is the optimal success probability achievable using only linear optics and vacuum ancillae.

When using the tunable c-phase gate for routing, several modifications of the setup have to be put in place [see Fig. 4(b)]: First, the PPG gate has to be replaced by a second c-phase gate set to the same phase shift as the first one. This c-phase gate would exercise the same transformation as described by Eq. (10), but with indices $1 \leftrightarrow 2$ swapped. Second, the transformation (HWP) performed on the control qubit between the two interaction gates is removed, and so is the NDF in upper arm ②. Finally, a generalized transformation in both arms ① and ② before the signal enters the c-phase gates has to be recalculated. This transformation reflecting the success probability of the c-phase gate reads

$$|H_1\rangle \to \frac{\sqrt{A_C}}{\sqrt{1 + A_C}}|H_1\rangle + \frac{1}{\sqrt{1 + A_C}}|V_1\rangle$$

in ① and

$$|V_2\rangle \to \frac{\sqrt{A_C}}{\sqrt{1 + A_C}}|H_2\rangle - \frac{1}{\sqrt{1 + A_C}}|V_2\rangle$$

in ②. This transformation assures the signal state independence of the routing procedure.

After incorporating these modifications, one can proceed in exactly the same manner as in Sec. II to reveal that the signal state just before impinging on the PBS$_2$ takes the form of

$$\frac{\alpha\sqrt{A_C}}{2\sqrt{2 + 2A_C}} \left[2\cos\theta + A_C e^{\iota\vartheta} \sin\theta(1 + e^{\iota\varphi}) \right] |H_1\rangle$$
$$+ \frac{\alpha e^{\iota\vartheta} \sin\theta \sqrt{A_C^3}}{2\sqrt{2 + 2A_C}}(1 - e^{\iota\varphi})|V_1\rangle \quad (11)$$

in the first arm ① and the form of

$$\frac{\beta\sqrt{A_C}}{2\sqrt{2 + 2A_C}} \left[2\cos\theta + A_C e^{\iota\vartheta} \sin\theta(1 + e^{\iota\varphi}) \right] |V_2\rangle$$
$$+ \frac{\beta e^{\iota\vartheta} \sin\theta \sqrt{A_C^3}}{2\sqrt{2 + 2A_C}}(1 - e^{\iota\varphi})|H_2\rangle \quad (12)$$

in the second arm ②. The Eqs. (11) and (12) indicate that the value of the phase shift φ imposed by the gate limits the routing ratio χ:

$$\tan\chi = \frac{A_C \sin\theta|1 - e^{\iota\varphi}|}{|2\cos\theta + A_C e^{\iota\vartheta} \sin\theta(1 + e^{\iota\varphi})|}.$$

For the sake of readability, we limit to $\vartheta = 0$ in the remaining part of this section. Thus, even for $\theta = \frac{\pi}{2}$ the routing ratio is bound by the relation

$$\chi_L(\varphi) \equiv \max\{\chi(\varphi, \theta)\}_\theta = \operatorname{atan}\left(\frac{1 - \cos\varphi}{\sin\varphi}\right) = \frac{\varphi}{2}, \quad (13)$$

where we have introduced the routing ratio limit χ_L for a given phase shift φ.

Using this definition, we can formulate the range of achievable routing ratios for a given phase shift φ to be $\chi \in [0; \chi_L]$ obtained when tuning monotonically the control qubit in the range $\theta \in [0; \frac{\pi}{2}]$. Note that, as expected, $\chi_L = 0$ for $\varphi = 0$ and $\chi_L = \frac{\pi}{2}$ for $\varphi = \pi$.

We can also easily find the success probability of the router by calculating the norm of the output state Eqs. (11) and (12).
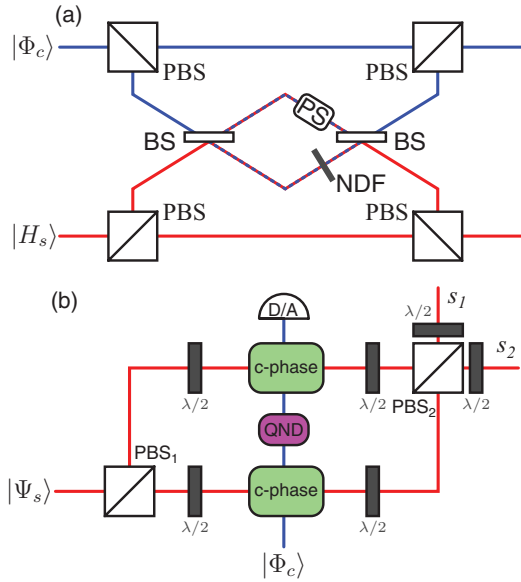
FIG. 4. (Color online) (a) Linear-optical scheme of a tunable c-phase gate. The interaction Mach-Zehnder interferometer replaces the fixed polarization dependent beam splitter (PDBS) in the original scheme. The phase shift imposed by the gate is tuned by setting specific values of phase shift (PS) and losses (NDF) in this interferometer (for more details see Ref. [31]). (b) Modified scheme of the router using two tunable c-phase gates. Red lines depict signal modes, while blue lines depict control modes.

This success probability function depends on both φ and θ. For a fixed value of φ we can find its minimum of

$$\min\{P_{\text{succ}}(\varphi,\theta)\}_{\theta} = \sqrt[3]{\frac{A_C^4}{2 + 2A_C}} \qquad (14)$$

always for $\theta = \frac{\pi}{2}$. On the other hand, the maximum success probability is obtained for different values of θ depending on the phase shift φ:

$$\theta|_{P_{\max}} = \frac{1}{2}\text{atan}\left[\frac{A_C(1 - \cos\varphi)}{1 - A_C^2}\right]. \qquad (15)$$

Both the success probability and the routing ratio limit are functions of the gate phase shift φ. To illustrate their mutual relation, we have plotted the success probability as a function routing limit in Fig. 5. In this figure, we show the maximum and minimum success probability together with the range between them for a given routing ratio limit. Observing this plot, we conclude that for sufficiently small values of routing ratio limit (e.g., $\chi_L = \frac{\pi}{8}$) the tunable c-phase gate offers increased success probability in comparison with the scheme proposed in the previous section. On the other hand, for larger routing ratio limits (closer to $\frac{\pi}{2}$), the former scheme does better since it uses only one c-phase gate together with a more efficient PPG gate.

IV. MULTIQUBIT ROUTING

So far we have only considered routing a single signal qubit using one control qubit. In principle, however, the device can route a chain of signal qubits making use of the same
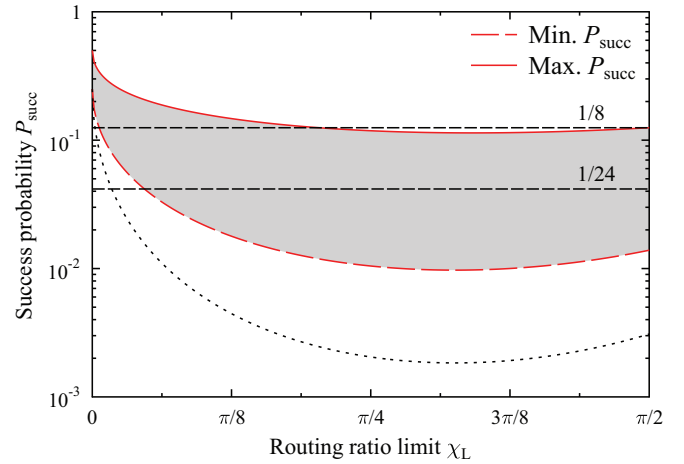

FIG. 5. (Color online) Maximum and minimum success probability of the router using two tunable c-phase gates depicted as functions of the routing ratio limit. The plot indicates that for sufficiently small values of routing ratio limit the tunable c-phase gate offers better performance than the scheme devised in the previous section (maximum and minimum success probability of the previous scheme is depicted using black dashed lines at $\frac{1}{8}$ and $\frac{1}{24}$). The dotted line shows the success probability if the standard state-independent c-phase gate is used instead of the generalized version.

control qubit. Figure 6 depicts the configuration for such multiqubit routing. In this model, two c-phase gates are used as in the previous section, but the control qubit is not detected immediately. After interacting with the first signal qubit, the control qubit presence is verified in a QND gate and then it is transferred back to the input of the router so it meets with the second signal qubit. After interacting with the last signal qubit, the control qubit is subjected to polarization analysis, thus projecting the state of all signal qubits.

Let us assume the state of the nth signal qubit to be

$$|\Psi_n\rangle = \alpha_n|H\rangle + \beta_n|V\rangle.$$

Thus, the state of the entire system can be expressed as

$$|\Psi_c\rangle \prod_n |\Psi_n\rangle_{\text{in}} = (\cos\theta|H\rangle + e^{i\vartheta}\sin\theta|V\rangle) \prod_n |\Psi_n\rangle_{\text{in}},$$

where the control qubit $|\Psi_c\rangle$ has been introduced as in previous sections. The procedure described in the previous paragraph
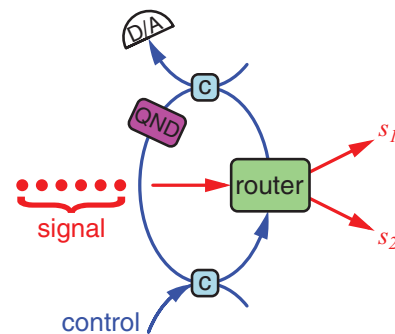

FIG. 6. (Color online) Scheme for multiqubit routing; c denotes the classical optical coupler. Red lines depict signal modes, while blue lines depict control modes.

then renders the state to

$$\cos\theta|H\rangle\prod_n|\Psi_n\rangle_{\text{out1}} + \frac{e^{\iota\vartheta}\sin\theta}{3}|V\rangle\prod_n|\Psi_n\rangle_{\text{out2}},$$

where out1 and out2 denote output ports of the router. Subsequent detection of the control qubit in the $|H\rangle \pm |V\rangle$ basis projects the state to the required form of

$$\cos\theta\prod_n|\Psi_n\rangle_{\text{out1}} + \frac{e^{\iota\vartheta}\sin\theta}{3}\prod_n|\Psi_n\rangle_{\text{out2}}.$$

Since the routing operation is probabilistic, the success probability of routing n qubits decreases exponentially with n. Considering the success probability of one run of the router to be P_{succ} (as calculated in previous section), the n-qubit router will perform with success probability

$$P_{\text{total}} = 2^{1-4n}\left(1 - \frac{8}{9}\sin^2\theta\right)^n.$$

It is worth noting that, apart from routing, this procedure can be used to generate the so-called noon states [37,38]. These states of the form of $(|N0\rangle + |0N\rangle)$, where N denotes the number of photons, are useful for instance in quantum metrology [39] or quantum lithography [40].

V. CONCLUSIONS

We have presented an all-linear-optical scheme for a fully quantum router. The router meets all the requirements presented in the introduction. This concept is more practical than some of the previously presented routers making use of experimentally difficult light-matter interaction or unrealistic strengths of nonlinear optical phenomena [21–24]. In contrast to previously published linear-optical schemes, our router provides genuine quantum routing being controlled by a qubit while not disturbing the state of the signal qubit (in contrast to [25]). Also, it only requires one control qubit to route a single signal qubit, making it more resource efficient (in contrast to [26]).

The proposed scheme operates with success probabilities ranging between $\frac{1}{8}$ and $\frac{1}{24}$ depending on the control qubit state.

We also discuss optimization of the success probability that can be reached by using tunable c-phase gates. The presented analysis shows how efficiency can be increased up to $\frac{1}{2}$ if only a small amplitude of the signal is needed to be sent to output port 2. Note also that detector efficiency just scales the success probability but does not change fidelity of the output.

We have also provided a recipe for a multiqubit router, in which the same control qubit is used to route the general number of signal qubits. In this case, the success probability of the procedure scales exponentially with the number of routed signal qubits.

While the entire scheme presented in this paper relies only on linear-optical quantum gates, it should be pointed out that the same setup can be constructed using gates based on nonlinear optical phenomena. Namely, the modified version as depicted in Fig. 4(b) can be transposed to nonlinear optics straightforwardly simply by replacing linear-optical c-phase gates by their nonlinear analogs. The benefit of such construction would be a significant improvement in success probability, since nonlinear c-phase gates can work deterministically. Also, the need for QND presence detection of the control qubit would become redundant. The nonlinear implementation of the c-phase gate is a heavily investigated topic currently facing severe experimental challenges [41–45].

[1] M. A. Nielsen and I. L. Chuang, *Quantum Computation and Quantum Information* (Cambridge University Press, Cambridge, 2000).

[2] D. Bouwmeester, A. Ekert, and A. Zeilinger, *The Physics of Quantum Information* (Springer, Heidelberg, 2001).

[3] A. Barenco, C. H. Bennett, R. Cleve, D. P. DiVincenzo, N. Margolus, P. Shor, T. Sleator, J. A. Smolin, and H. Weinfurter, Phys. Rev. A **52**, 3457 (1995).

[4] J. L. O'Brien, G. J. Pryde, A. G. White, T. C. Ralph, and D. Branning, Nature (London) **426**, 264 (2003).

[5] G. Brassard, Nat. Phys. **1**, 2 (2005).

[6] D. Medhi and K. Ramasamy, *Network Routing: Algorithms, Protocols, and Architectures* (Morgan Kaufmann, San Francisco, 2007).

[7] B. E. A. Saleh, and M. C. Teich, *Fundamentals of Photonics*, 2nd ed. (Wiley, New York, 2007).

[8] H. J. Kimble, Nature (London) **453**, 1023 (2008).

[9] N. Gisin, G. Ribordy, W. Tittel, and H. Zbinden, Rev. Mod. Phys. **74**, 145 (2002).

[10] V. Scarani, H. Bechmann-Pasquinucci, N. J. Cerf, M. Dušek, N. Lütkenhaus, and M. Peev, Rev. Mod. Phys. **81**, 1301 (2009).

[11] J. L. Jackel, E. M. Vogel, and J. S. Aitchison, Appl. Opt. **29**, 3126 (1990).

[12] J. Ruiqiang *et al.*, Opt. Express **19**, 20258 (2011).

[13] J. Doyle and Jennifer DeHaven Carroll, *Routing TCP/IP 1*, 2nd ed. (Cisco Press, Indianopolis, 2005).

[14] V. Bužek and M. Hillery, Phys. Rev. A **54**, 1844 (1996).

[15] V. Scarani, S. Iblisdir, N. Gisin, and A. Acin, Rev. Mod. Phys. **77**, 1225 (2005).

[16] N. J. Cerf and J. Fiurášek, in *Progress in Optics*, edited by E. Wolf (Elsevier, Amsterdam, 2006), Vol. 49, p. 455.

[17] H. Fan, Y.-N. Wang, L. Jing, J.-D. Yue, H.-D. Shi, Y.-L. Zhang, and L.-Z. Mu, arXiv:1301.2956v3.

[18] K. Bartkiewicz and A. Miranowicz, Phys. Rev. A **82**, 042330 (2010).

[19] K. Lemr, K. Bartkiewicz, A. Černoch, J. Soubusta, and A. Miranowicz, Phys. Rev. A **85**, 050307(R) (2012); K. Bartkiewicz, K. Lemr, A. Černoch, J. Soubusta, and A. Miranowicz, Phys. Rev. Lett. **110**, 173601 (2013).

[20] P. Kok *et al.*, Rev. Mod. Phys. **79**, 135 (2007).

[21] D. Zueco, F. Galve, S. Kohler, and P. Hänggi, Phys. Rev. A **80**, 042303 (2009).

[22] T. Aoki, A. S. Parkins, D. J. Alton, C. A. Regal, B. Dayan, E. Ostby, K. J. Vahala, and H. J. Kimble, Phys. Rev. Lett. **102**, 083601 (2009).

[23] Io-Chun Hoi, C. M. Wilson, G. Johansson, T. Palomaki, B. Peropadre, and P. Delsing, Phys. Rev. Lett. **107**, 073601 (2011).

[24] M. A. Hall, J. B. Altepeter, and P. Kumar, Phys. Rev. Lett. **106**, 053901 (2011).

[25] X.-Y. Chang, Y.-X. Wang, C. Zu, K. Liu, and L.-M. Duan, arXiv:1207.7265v1.

[26] K. Lemr and A. Černoch, Opt. Comm. **300**, 282 (2013).

[27] E. Halenková *et al.*, App. Opt. **51**, 474 (2012).

[28] J. Eisert, K. Jacobs, P. Papadopoulos, and M. B. Plenio, Phys. Rev. A **62**, 052317 (2000).

[29] T. B. Pittman, M. J. Fitch, B. C. Jacobs, and J. D. Franson, Phys. Rev. A **68**, 032316 (2003).

[30] K. Kieling, J. L. O'Brien, and J. Eisert, New J. Phys. **12**, 013003 (2010).

[31] K. Lemr, A. Černoch, J. Soubusta, K. Kieling, J. Eisert, and M. Dušek, Phys. Rev. Lett. **106**, 013602 (2011).

[32] K. Lemr and A. Černoch, Phys. Rev. A **86**, 034304 (2012).

[33] M. Bula, K. Bartkiewicz, A. Černoch, and K. Lemr, Phys. Rev. A **87**, 033826 (2013).

[34] G. Vidal, L. Masanes, and J. I. Cirac, Phys. Rev. Lett. **88**, 047905 (2002).

[35] M. Mičuda, M. Ježek, M. Dušek, J. Fiurášek, Phys. Rev. A **78**, 062311 (2008).

[36] M. Miková, H. Fikerová, I. Straka, M. Mičuda, J. Fiurášek, M. Ježek, and M. Dušek, Phys. Rev. A **85**, 012305 (2012).

[37] J. Fiurášek, Phys. Rev. A **65**, 053818 (2002).

[38] M. Mitchell, J. Lundeen, and A. Steinberg, Nature (London) **429**, 161 (2004).

[39] T. Nagata, R. Okamoto, J. L. O'Brien, K. Sasaki, and S. Takeuchi, Science **316**, 726 (2007)

[40] G. Björk, L. L. Sánchez-Soto, and J. Söderholm, Phys. Rev. Lett. **86**, 4516 (2001).

[41] S. E. Harris and L. V. Hau, Phys. Rev. Lett. **82**, 4611 (1999).

[42] K. Nemoto and W. J. Munro, Phys. Rev. Lett. **93**, 250502 (2004).

[43] W. J. Munro, K. Nemoto, and T. P. Spiller, New. J. Phys. **7**, 137 (2005).

[44] Q. Lin and J. Li, Phys. Rev. A **79**, 022301 (2009).

[45] X. M. Xiu, L. Dong, H. Z. Shen, Y. J. Gao, and X. X. Yi, J. Opt. Soc. Am. B **30**, 589 (2013).